A Robust Descriptor for Color Texture Classification Under Varying Illumination

Tamiris Trevisan Negri[1,2,3], Fang Zhou[2], Zoran Obradovic[2] and Adilson Gonzaga[1]
[1]*Department of Electrical and Computer Engineering, University of São Paulo, São Carlos, Brazil*
[2]*Center for Data Analytics and Biomedical Informatics, Temple University, Philadelphia, U.S.A.*
[3]*Federal Institute of Education, Science and Technology of São Paulo, Araraquara, Brazil*
tamirisnegri@usp.br, {fang.zhou, zoran.obradovic}@temple.edu, agonzaga@sc.usp.br

Keywords: Color Texture, Texture Description, Illumination, Local Descriptors.

Abstract: Classifying color textures under varying illumination sources remains challenging. To address this issue, this paper introduces a new descriptor for color texture classification, which is robust to changes in the scene illumination. The proposed descriptor, named Color Intensity Local Mapped Pattern (CILMP), incorporates relevant information about the color and texture patterns from the image in a multiresolution fashion. The CILMP descriptor explores the color features by comparing the magnitude of the color vectors inside the RGB cube. The proposed descriptor is evaluated on nine experiments over 50,048 images of raw food textures acquired under 46 lighting conditions. The experimental results have shown that CILMP performs better than the state-of-the-art methods, reporting an increase (up to 20.79%) in the classification accuracy, compared to the second-best descriptor. In addition, we concluded from the experimental results that the multiresolution analysis improves the robustness of the descriptor and increases the classification accuracy.

1 INTRODUCTION

Texture analysis is an important and widely explored field in computer vision. There are many existing works studying a variety of models to describe textures, most of them designed for gray-scale images. Although color is often ignored by many texture descriptors, some works have shown the importance of color in the process of describing a texture (Setchell and Campbell, 1999; Drimbarean and Whelan, 2001; Palm, 2004; Maenpaa and Pietikinen, 2004; Bianconi et al., 2011).

In the last two decades, several descriptors were developed to incorporate color information in different tasks, such as classification, segmentation and recognition. Statistical approaches based on co-occurrence matrices together with color description are used for image retrieval and texture classification (Arvis et al., 2004; Vadivel et al., 2007). Wavelets and Gabor Filters were also investigated for that purpose (Maenpaa and Pietikinen, 2004; Campbell et al., 1996; de Wouwer et al., 1999; Sengur, 2008; Palm and Lehmann, 2002; Jain and Healey, 1998).

Local texture descriptors, such as local binary pattern (LBP) (Ojala et al., 1996; Ojala et al., 2002), have been extended to be applied to color textures. Opponent color local binary pattern (OCLBP) combines LBP histograms and opponent color texture features for facial recognition (Chan et al., 2007). Intensity color contrast descriptor (ICCD) and local color contrast (LCC) (Cusano et al., 2013; Cusano et al., 2014) combine the LBP histogram with information associated to the color contrast of the image.

Experiments performed by Maenpaa and Pietikainen (Maenpaa and Pietikinen, 2004) showed that color descriptors perform better than the gray-scale descriptors for texture classification tasks. However, the same work showed that the color texture descriptors are negatively affected by varying illumination conditions.

To overcome the issue of varying illumination, some authors proposed color normalization algorithms as a pre-processing step for texture description methods (Kandaswamy et al., 2012; Cusano et al., 2014; Cusano et al., 2016). However, it has been shown that the normalization requires an extra computational cost only resulting in improvement in very specific conditions (Cusano et al., 2016).

In this paper we propose a new color texture descriptor robust to variations on the illumination source. The proposed descriptor, named Color Intensity Local Mapped Pattern (CILMP), extends the

Negri, T., Zhou, F., Obradovic, Z. and Gonzaga, A.
A Robust Descriptor for Color Texture Classification Under Varying Illumination.
In *Proceedings of the 12th International Joint Conference on Computer Vision, Imaging and Computer Graphics Theory and Applications (VISIGRAPP 2017) - Volume 4: VISAPP*, pages 378-388
ISBN: 978-989-758-225-7

local mapped pattern descriptor (LMP) presented in (Ferraz et al., 2014) for color texture classification. CILMP incorporates relevant information about the color and texture patterns from the image. This information can be extracted jointly or separately. Studies about the human visual system show that texture and color information are processed separately by the human brain (Poirson and Wandell, 1996). In (Maenpaa and Pietikinen, 2004), the authors also concluded that color and texture are separate phenomena and should be treated individually. Therefore, the proposed descriptor processes color and texture information separately to make it close to human perception.

The proposed descriptor incorporates color information using the magnitude of the color vector inside the RGB cube. Both color and texture information are processed separately from different texture resolutions to capture information from a range of frequency patterns. The local patterns obtained from each resolution are mapped to a histogram using a parametric function. In this paper, we apply a genetic algorithm to tune the parameters simultaneously in order to optimize the multiresolution analysis.

The proposed descriptor is evaluated on a large dataset composed of 50,048 images of raw food textures designed especially to investigate the robustness of texture descriptors when the scene illumination changes. The experimental results indicate that combining different resolutions makes the descriptor more robust, increasing the classification accuracy. Moreover, CILMP outperforms the existing descriptors considered in the comparison.

The remaining of this paper is organized as follow: Section 2 provides a review of the local mapped pattern descriptor and an extension of the method designed for multiresolution analysis. Section 3 presents the proposed descriptor CILMP. The experiments are reported and discussed in Section 4 and, finally, we conclude the paper in Section 5.

2 LOCAL MAPPED PATTERN

In this section we first provide a brief description of the local mapped pattern (LMP) descriptor (Ferraz et al., 2014). Then, we present a natural extension of this approach for circular neighborhoods, which allows a multiresolution analysis.

The LMP descriptor was proposed by Ferraz et al. (Ferraz et al., 2014) and originally designed for grayscale images. Let us consider a 3×3 local pattern as shown in Fig. 1. Assuming that g_c is the central pixel in the local pattern, the LMP considers the differences between g_c and its neighboring pixels g_i, $i = 1, \ldots, 8$, as the argument of a weighting function which maps each difference to a histogram bin.

g_1	g_2	g_3
g_4	g_c	g_5
g_6	g_7	g_8

Figure 1: Local Pattern 3×3.

A local pattern from a $v = W \times W$ squared neighborhood can be mapped to a histogram bin h_b according to

$$h_b = \text{round}\left(\frac{\sum_{i=1}^{v-1} f_{g_i} M(i)}{\sum_{i=1}^{v-1} M(i)} (B-1)\right), \qquad (1)$$

where f is the mapping function applied to the difference between each neighbor g_i and the central pixel g_c, B is the number of histogram bins and M is a weighting matrix of predefined values for each pixel position within the neighborhood. The mapping function, number of histogram bins and weighting matrix can be set according to the application. In (Ferraz et al., 2014) the mapping function is defined as the sigmoid function, given by

$$f_{g_i} = \frac{1}{1 + \exp\left(\frac{-[g_i - g_c]}{\beta}\right)}, \qquad (2)$$

where β is the steepness of the curve and $[g_i - g_c]$ is the difference between the central pixel g_c and its neighbors g_i $(i = 1, \ldots, v-1)$.

2.1 Sampled Local Mapped Pattern

The LMP methodology can be easily extended to circular neighborhoods around the central pixel. Given the number P of neighboring pixels, g_p corresponds to the value of each sampled pixel P, equally spaced in a circle of radius R $(R > 0)$, forming a set of neighbors of circular symmetry, in a counterclockwise order as shown in Fig. 2.

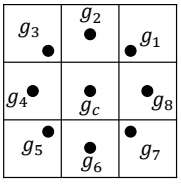

Figure 2: Neighbors of a circular symmetry, where $P = 8$ and $R = 1$.

Assume that the corresponding central pixel g_c is located at $(x,y) = (0,0)$, the coordinates of each neighbor pixel g_p are $(x,y) = (-Rsin(2\pi p/P), Rcos(2\pi p/P))$. The pixel values that are not located in the exact center of each pixel are estimated through interpolation, inspired by (Ojala et al., 2002).

This new version of LMP, called sampled-local mapped pattern (S-LMP), is capable of sampling several resolutions of radius (R) and number of neighbors (P). The combination of different neighborhood configurations (P,R) leads to a multiresolution analysis which increases the power of the descriptor to extract relevant features from the texture.

Each S-LMP pattern defined by P samples and radius R is mapped to a histogram bin h_b using Eq. (3), where B is the number of histogram bins and f is the sigmoid mapping function given by Eq. (2) in which β is the steepness of the curve. A weighting matrix is not used in this approach, only the number of the pixel samples P, which guarantees the rotation invariant characteristic.

$$h_b = \text{round}\left(\frac{\sum_{p=1}^{P} f_{g_p}}{P}(B-1)\right). \qquad (3)$$

3 COLOR INTENSITY LOCAL MAPPED PATTERN

The CILMP model is a parametric descriptor that combines color and texture information in several resolutions to get high accuracy in classification tasks under varying illumination. In this section, we introduce how CILMP incorporates texture and color information from the images to the feature vectors, and propose the application of a genetic algorithm to tune the descriptor parameters in order to optimize the multiresolution analysis.

3.1 Feature Extraction

In CILMP, the texture information is extracted from the image luminance by the S-LMP descriptor presented in Section 2.1. To get a multiresolution analysis, the descriptor is applied using different neighborhood configurations. The obtained histograms from each neighborhood configuration are concatenated to form the CILMP texture feature vector.

For the extraction of color information we propose a novel approach based on the magnitude of the color vectors inside the RGB cube. On a three-dimensional color space, each axis represents a channel, and therefore each color can be represented as a point inside the 3-D space. For example, on the RGB color space, a color is characterized by its primary components red, green and blue (Gonzalez and Woods, 2008). A local 3×3 pattern of color texture is a three-dimensional matrix where each pixel is described by three coordinates $g_i = (R_i, G_i, B_i)$.

To extend the S-LMP descriptor for color images, the difference between the squared magnitudes of vectors in the RGB space is used as input of the sigmoid function

$$f_{g_p} = \frac{1}{1+\exp\left(\frac{-\left(||g_p||^2 - ||g_c||^2\right)}{\beta}\right)}, \qquad (4)$$

where β is the steepness of the curve, g_c is the central pixel of the local pattern and g_p is a neighbor of g_c. Symmetric circular neighborhoods are used to allow a multiresolution analysis. The patterns are mapped to a histogram bin h_b according to Eq. (3). Figure 3 shows an RGB texture and its S-LMP map obtained considering the sigmoid function presented by Eq. 4, eight neighbors and radius equal to two.

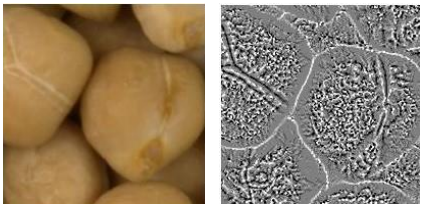

Figure 3: Example of an RGB texture and its S-LMP map.

We apply the descriptor to color textures using different neighborhood configurations. The obtained histograms are concatenated to the texture histograms provided by the S-LMP, forming the CILMP feature vector.

Fig. 4 shows the multiresolution analysis performed by the CILMP: different radius and number of neighbors are used to extract texture information from the luminance map and color information from the RGB channels. Note that, for example, the neighborhood $(P,R) = (24,5)$ just considers the pixel values which are distant five positions from the central pixel. Combining different neighborhood resolutions allows the descriptor to extract information from a larger area, including more features in the feature vector.

3.2 Genetic Algorithm for Parameter Tuning

The β parameter used in the sigmoid mapping function (Eq. 4) is related to the curve slope. It changes

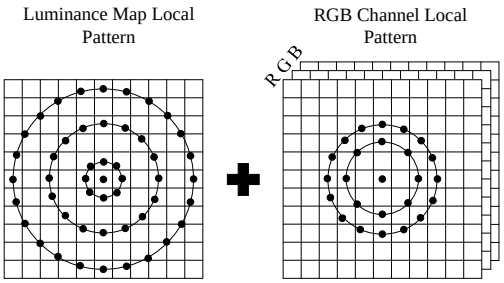

Figure 4: Example of a multiresolution analysis by the CILMP using five configurations: $(8,1)+(16,3)+(24,5)$ for the luminance map and $(8,2)+(16,3)$ for the RGB channels.

the sensitivity of the method to the nuances in the image and directly affects the descriptor performance. Note that $\beta \in \mathbb{R}$, $\beta \neq 0$, in Eq. (2) . Since we are not considering the absolute value in the argument of the sigmoid function, we fix $\beta > 0$ to keep the curve direction.

Fig. 5 shows the sigmoid curve behavior for a range of β values. Small β values quickly saturate the pixel differences to 0 or 1, resembling the LBP (Ojala et al., 1996; Ojala et al., 2002). Large β values approximate the curve to a straight line parallel to the abscissas axis, so that the pixel differences are mapped to values around 0.5.

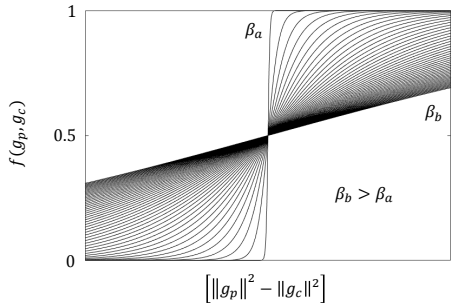

Figure 5: Sigmoid curve behavior for a range of β values. Small β values quickly saturate the pixel differences to 0 or 1. Large β values make the curve more flat.

For each neighborhood configuration we adopted a different value of β. The CILMP showed in Fig. 4, for example, uses three configurations to extract texture features and two for color features. So, five β parameters need to be tuned.

Since the parameters from the five neighborhoods influence each other when they are combined to form the CILMP feature vector, we propose to adjust them, simultaneously, by using genetic algorithm. The accuracy is used as an objective function to be maximized.

4 EXPERIMENTS

4.1 Experimental Setup

In this work, the research problem is formulated as a classification problem, that is, to predict which class an image belong to. To evaluate the performance of the CILMP descriptor we used the Raw Food Texture (RawFooT) database, which was designed by Cusano et al. (Cusano et al., 2016) specially to investigate the robustness of color texture descriptors against lighting changes in classification problems. The database consists of 68 raw food textures of size 800×800 pixels, acquired under 46 lighting conditions which differ in direction, color, temperature, intensity and combination of these factors. The original images were divided into 16 non-overlapping samples of 200×200 pixels: 8 samples for training and 8 samples for test. There are 68 classes in this dataset and the goal is to classify a sample in the correct class. The total number of samples is $68 \times 46 \times 16 = 50048$, half of them for training and the remaining for test. The 46 lighting conditions are listed below and illustrated in Fig. 6.

- **(1-4) Intensity variations:** Daylight at 6500 K and four intensity levels: 100%, 75%, 50% and 25%;
- **(5-13) Light direction:** Daylight at 6500 K and nine incident angles: 24°, 30°, 36°, 42°, 48°, 54°, 60° and 90°;
- **(14-25) Daylight temperature:** Daylight at twelve different color temperatures from 4000 K to 9500 K with steps of 500 K.
- **(26-31) LED temperature:** LED sources with six different color temperatures: 2700 K, 3000 K, 4000 K, 5000 K, 5700 K and 6500 K;
- **(32-40) Color and direction:** combinations of three colors (Daylight 6500 K, Daylight 9500 K and LED 2700 K) and three incidence directions (24°, 60° and 90°);
- **(41-43) Multiple illuminants:** combinations of two illuminants with different colors among Daylight 6500 K, Daylight 9500 K and LED 2700 K;
- **(44-46) Primary colors:** pure red, green and blue illuminants.

We performed the nine texture classification tasks, same as (Cusano et al., 2016), using the RawFooT database. Each task contains several subsets composed by training and test images taken under the light condition to be analyzed. For example, let us consider task 2, which involves four different lighting intensities. If we assign the training samples acquired under

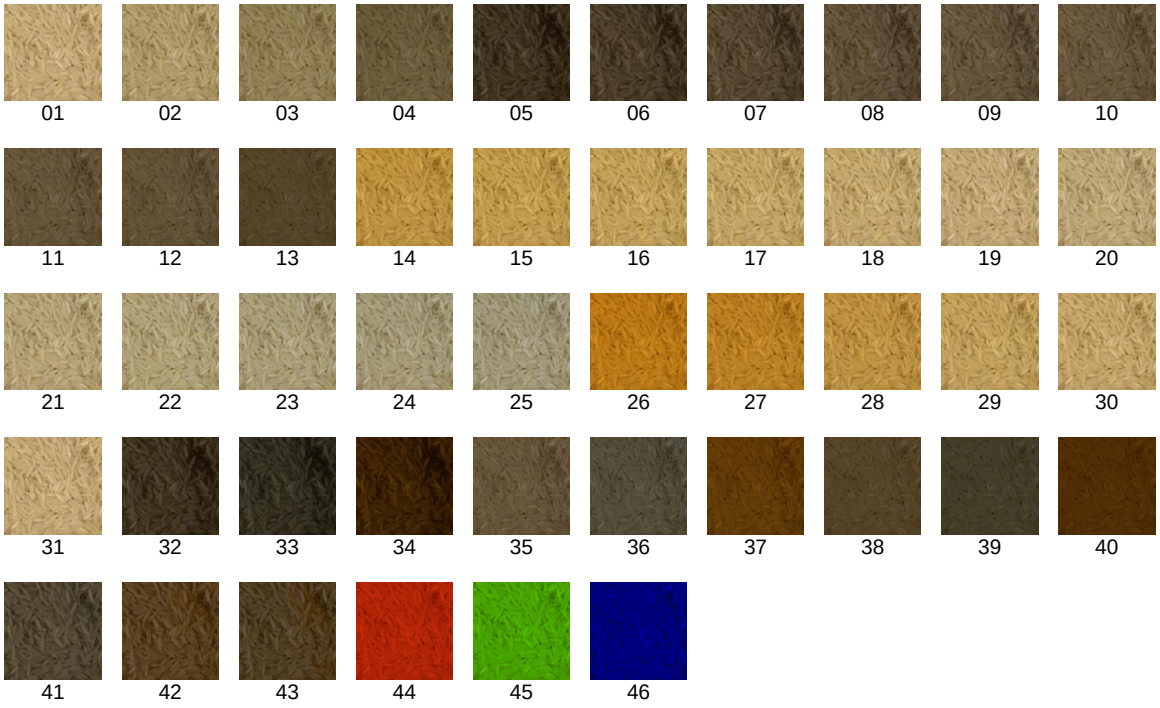

Figure 6: Example of one of the textures (rice) in the Raw Food Texture database imaged under the 46 lighting conditions as described in Section 4.1.

a light source of intensity level 100% as the training group, we can form 3 subsets (training, test) considering the test samples taken under the other 3 intensity levels: (100%, 75%), (100%, 50%) and (100%, 25%). Since there are four intensity levels, we can form $4 \times 3 = 12$ subsets. Below is the brief description of the nine tasks.

1. **No variations:** 46 subsets. For each subset, training and test samples were taken under the same light conditions.
2. **Light intensity:** 12 subsets, each one composed of training and test samples taken under different light intensities.
3. **Light direction:** 72 subsets, each one composed of training and test samples taken under different light directions.
4. **Daylight temperature:** 132 subsets, each one composed of training and test sets with images taken under different color temperatures.
5. **LED temperature:** 30 subsets, each one composed of training and test sets with images taken under different LED light temperatures.
6. **Daylight vs. LED:** 72 subsets combining the twelve daylight temperatures with the six LED temperatures.
7. **Temperature or direction:** 72 subsets combining the light conditions 32 to 40, where the training and test samples differ in color or direction or both, color and direction.
8. **Temperature and direction:** 36 subsets combing the light conditions 32 to 40, where the training and test sets samples differ in both color and direction.
9. **Multiple illuminats:** 6 subsets combining the light conditions 41 to 43.

For each task, the CILMP descriptor is applied to both training and test samples to extract feature vectors. The dissimilarity between training and test samples, is measured by calculating the distance of the feature vector from the test sample and the feature vector of the training sample using the L_1 distance $D(S,M) = \sum_{b=1}^{B_t} |S_b - M_b|$, where S is the feature vector of a training sample, M is the feature vector of a test sample and B_t stands for the number of bins in the feature vector.

In all the experiments we applied the K-nearest neighbor classifier $(K = 1)$ to estimate the label of the test images: the feature vector of each test sample is compared to all feature vectors of the training samples, and the class of the training sample which provides the smallest dissimilarity is considered as the prediction of the test sample. Since there are several

subsets in each classification task, the performance of the method is evaluated using three measurements: the average over the accuracies provided by each subset classification, the minimum accuracy among them and the average rank of the descriptor over the nine tasks.

In this work, the CILMP model uses five neighborhood configurations: three configurations for the luminance map – $(8,1)$, $(16,3)$ and $(24,5)$ and two configurations for the RGB channels– $(8,2)$ and $(16,3)$ (as shown in Fig. 4). Considering the pixel intensity variation is larger in the luminance image, we use more resolutions to extract texture information. Preliminary experiments showed that these five neighborhood configurations are enough to get high accuracy. Increasing the number of neighborhoods configurations produces similar results but increases the size of the feature vector, therefore increasing computational cost.

The number of histogram bins B was set to 256 for each neighborhood configuration. So the CILMP feature vector has $256 \times 5 = 1280$ positions.

4.2 Performance of the Individual Descriptors

First, we analyze the performance of the individual descriptors and the influence of the β parameter in the classification rate. We selected a training and a test set which contains images taken under multiple light sources with different lighting conditions. Fig. 7 and Fig. 8 show the classification accuracies when the β parameter varies between $(0,5]$ for each neighborhood configuration separately. Since f is not defined if $\beta = 0$, we chose 10^{-10} as the minimum value for β.

Fig. 7 and Fig. 8 show that the optimal β is within $(0,1]$ for all the proposed configurations. Based on that, we analyze the β behavior only in that interval. Table 1 shows the worst and best accuracies for each neighborhood configuration, and the corresponding β values.

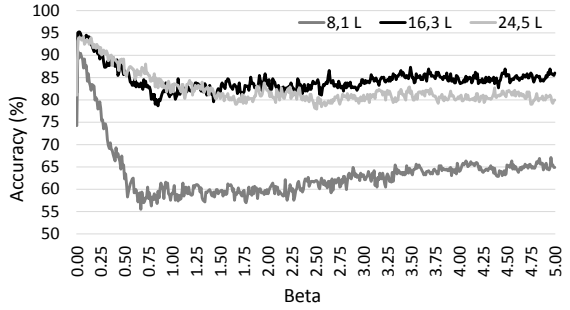

Figure 7: Accuracy obtained from the β parameters between $(0,5]$ considering different configurations of neighborhoods for luminance maps.

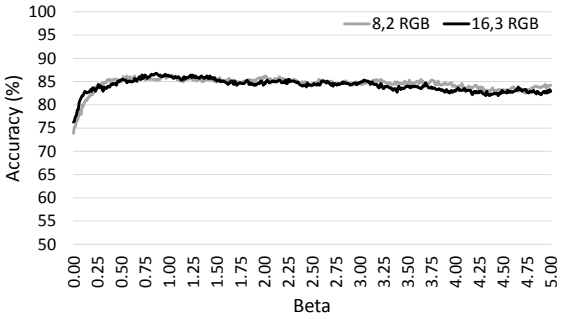

Figure 8: Accuracy obtained from the β parameters between $(0,5]$ considering different configurations of neighborhoods for RGB channels.

Table 1: Lowest and highest classification accuracy (%) and the respective β ($0 < \beta \leq 1$) for each configuration of (P,R).

(P,R)	lowest acc. (β)	highest acc. (β)
$(8,1)$ L	55.51 (0.67)	90.99 (0.01)
$(16,3)$ L	78.68 (0.85)	95.22 (0.02)
$(24,5)$ L	81.07 (10^{-10})	94.12 (0.07)
$(8,2)$ RGB	73.90 (10^{-10})	86.40 (0.71)
$(16,3)$ RGB	76.29 (10^{-10})	86.76 (0.86)

The configuration $(P,R) = (16,3)$ applied to the image luminance presents higher accuracy (95.22%) than the others.The lowest accuracy for $(P,R) = (16,3)$ is 78.68%, so the difference between the lowest and highest reaches 16.54%. Combining the five configurations and using the β values, with which individual configuration gives the result of highest accuracy, produce the classification accuracy 96.32%. Moreover, using β values, with which individual descriptor produces lowest accuracy, produce 95.22% of accuracy, which is better than the performance of the individual descriptors. Therefore, five descriptors together produces much better results than the individual one, and thus, is more robust to classify texture acquired under different light sources.

4.3 Performance of CILMP

In this section, we describe the performance of the proposed CILMP descriptor. The parameters presented in Table 1 are tuned separately, however, they can influence each other on the feature vector comparison. Therefore, to get the optimal β values used in the CILMP model, we apply a genetic algorithm to tune all the parameters simultaneously. We consider $\beta \in (0,1]$ (based on results of Fig. 7 and Fig. 8) and the accuracy was used as objective function to be maximized. The maximum accuracy reported by the genetic algorithm is 97.98%. So, we can conclude

that the classification rate is increased by tuning all the parameters together.

After some preliminary experiments, we noticed that the β parameters could be adjusted by using a few images in the tuning process: just two samples from each class are enough in the tuning set, and the CILMP could achieve a good performance. Based on that, a tuning set is generated by randomly selecting two samples per class from the 25024 training images. Since the database involves 68 classes, the tuning set contains 168 images. The set of the five β parameters that produces the highest accuracy in the tuning set is used on the CILMP descriptor to perform the classification tasks. To guarantee that the images chosen are not affecting the results, we repeated the experiments, using seven different sets of β. One of the β values set is $[0.08, 0.13, 0.98, 0.17, 0.14]$ for the neighborhoods (8,1) L, (16,3) L, (24,5) L, (8,2) RGB and (16,3) RGB respectively.

Table 2 reports the average and standard deviation of the average accuracy obtained for the nine tasks presented in Subsection 4.1. We notice that the standard deviation is small for all the tasks, so that the random selection of images does not affect the classification accuracy.

Table 2: Average over the average accuracy (%) and standard deviation from seven tuning sets obtained by CILMP.

Light Condition Changing	Avg. Acc.	Std. Dev.
No variations	97.98	0.0952
Light intensity	79.10	2.3215
Light direction	63.70	1.1156
Daylight temperature	97.09	0.1556
LED temperature	95.04	0.1682
Daylight vs. LED	93.95	0.0992
Temperature or direction	42.87	0.8114
Temperature and direction	28.72	0.9149
Multiple illuminant	95.59	0.3341

We compare the obtained accuracy using CILMP to the results provided by Cusano et. al. (Cusano et al., 2016) using other baselines. Among the methods presented in (Cusano et al., 2016), we selected for comparison the traditional texture descriptors designed for texture analysis, which is the focus of this paper.

Table 3 reports a rank of the performance of each descriptor over the nine tasks. Fig. 9 to 17 show the average accuracy obtained for each descriptor according to the task. Fig. 18(a) shows the improvement achieved by CILMP over the other methods in terms of average accuracy.

The accuracy presented in Fig. 9 to 17 is the average between the accuracies provided by several subsets in a task, as explained in Subsection 4.1. We also evaluate the descriptor considering the minimum accuracy presented for each task. The improvement in the minimum accuracy performed by CILMP, for each task, is reported in Fig. 18(b). The data used in Fig. 9-18 and Table 3 are provided by (Cusano et al., 2016).

As expected, most of the descriptors achieve high accuracy when there are no changes in the illumination condition (task 1). Descriptors that were applied to both color and luminance channels, such as LBP, histogram, co-occurrence matrix, wavelet transform and Gabor filter, performed better when the color was considered, confirming the importance of color in the process of describing a texture. CILMP achieves the best accuracy (97.98%) for this task, with an improvement varying between 0.74% and 79.30% (Fig. 18(a)). The minimum accuracy achieved by the proposed method is close to the best, as presented in Fig. 18(b).

CILMP also outperforms the other methods for task 2, which considers changes in the light intensity. The improvements in the average accuracy provided by the proposed descriptor are between 0.35% and 75.78%. We can also notice from Fig. 18(b) that the minimum accuracy performed by CILMP is very close to the best minimum.

When the light direction changes (task 3), CILMP achieves average accuracy of 63.70%, the 3*rd* best result for this task, 2.00% smaller than highest accuracy. This is the only task in which the proposed descriptor does not outperform the other methods in terms of average accuracy.

CILMP achieves excellent results for changes in temperature when natural daylight (97.09%) and LED lights (95.04%) are considered. High accuracy is also reported when we compare images acquired under daylight source to the images acquired under LED light (93.65%). For these three tasks (tasks 4, 5 and

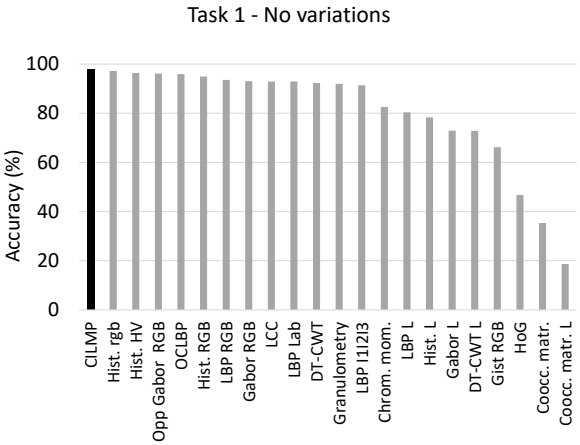

Figure 9: Average accuracy (%) obtained by CILMP and other texture descriptors for task 1.

Table 3: Rank of performance of the proposed method and others texture descriptors.

Descriptor	Reference	Rank
CILMP	Our model	1.22
LCC	(Cusano et al., 2014; Cusano et al., 2016)	4.22
LBP Lab	(Ojala et al., 2002; Cusano et al., 2016)	5.33
OCLBP	(Maenpaa and Pietikinen, 2004; Cusano et al., 2016)	5.89
LBP L	(Ojala et al., 2002; Cusano et al., 2016)	6.56
LBP RGB	(Ojala et al., 2002; Cusano et al., 2016)	6.67
LBP $I_1I_2I_3$	(Ojala et al., 2002; Cusano et al., 2016)	7.11
Gabor RGB	(Bianconi et al., 2011; Cusano et al., 2016)	9.11
Gabor L	(Bianconi et al., 2011; Cusano et al., 2016)	9.44
Opp Gabor RGB	(Jain and Healey, 1998; Cusano et al., 2016)	10.89
Granulometry	(Hanbury et al., 2005; Cusano et al., 2016)	11.56
DT-CWT	(Bianconi et al., 2011; Cusano et al., 2016)	11.89
Hist. H V	(Cusano et al., 2016)	12.56
Hist. *rgb*	(Cusano et al., 2016)	12.78
Gist RGB	(Oliva and Torralba, 2001; Cusano et al., 2016)	13.00
Hist. RGB	(Cusano et al., 2016)	14.78
Chrom. mom.	(Paschos, 2000; Cusano et al., 2016)	15.56
DT-CWT L	(Bianconi et al., 2011; Cusano et al., 2016)	16.22
HoG	(Junior et al., 2009; Cusano et al., 2016)	17.22
Hist. L	(Cusano et al., 2016)	18.33
Coocc. matr.	(Cusano et al., 2016)	20.67
Coocc. matr. L	(Cusano et al., 2016)	22.00

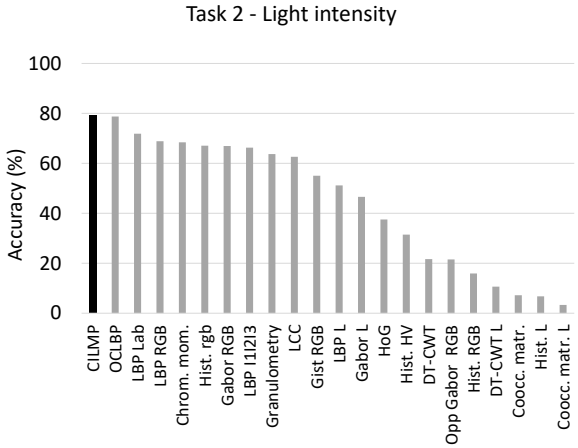

Figure 10: Average accuracy (%) obtained by CILMP and other texture descriptors for task 2.

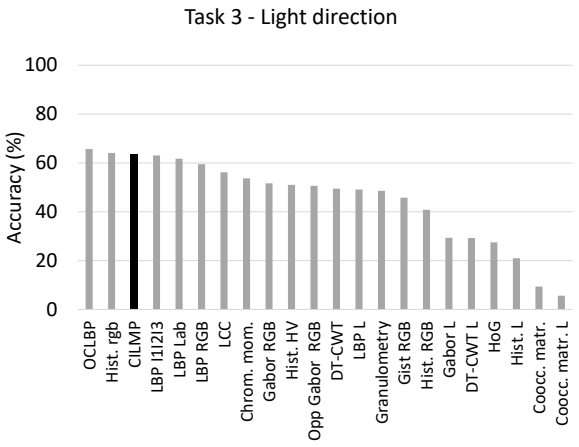

Figure 11: Average accuracy (%) obtained by CILMP and other texture descriptors for task 3.

6), the proposed descriptor performs the best, outperforming the 2*nd* best (LCC descriptor) by large margins: 8.33% for task 4, 20.79% for task 5 and 15.13% for task 6. Fig. 12-14 and Fig. 18(b) show that CILMP also reports improvements larger than 18.20%, 24.45% and 25.09%, respectively, in terms of minimum accuracy.

Tasks 7 and 8 include variations in the temperature or/and direction of the light sources. We notice that all the descriptors achieve poor performance in these tasks. The best accuracy is achieved by CILMP with 42.87% of accuracy when either temperature or direction varies and 28.72% when both temperature and direction vary. CILMP also provided the best minimum rate for both tasks. It is clear that accounting for changes in the direction of the light source is the most challenging condition as shown by tasks 3, 7 and 8.

CILMP also has a superior performance in the last task, when the images are taken under multiple illuminants and they vary between training and test samples. The proposed descriptor achieves the best average accuracy (95.59%) and the best minimum. The

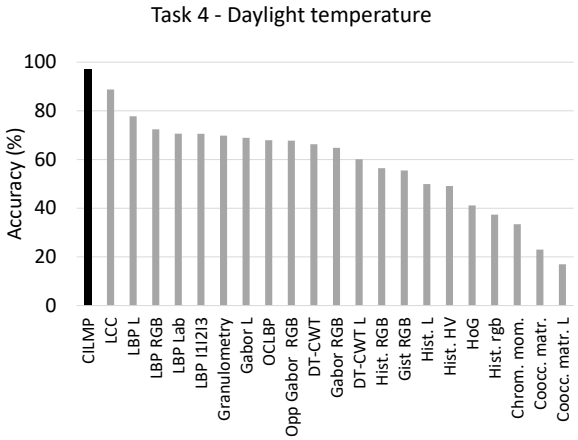

Figure 12: Average accuracy (%) obtained by CILMP and other texture descriptors for task 4.

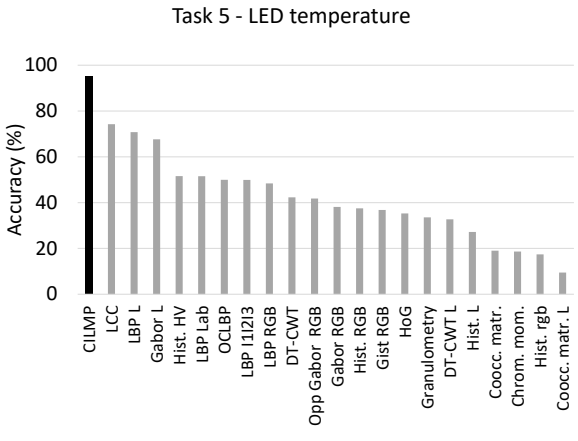

Figure 13: Average accuracy (%) obtained by CILMP and other texture descriptors for task 5.

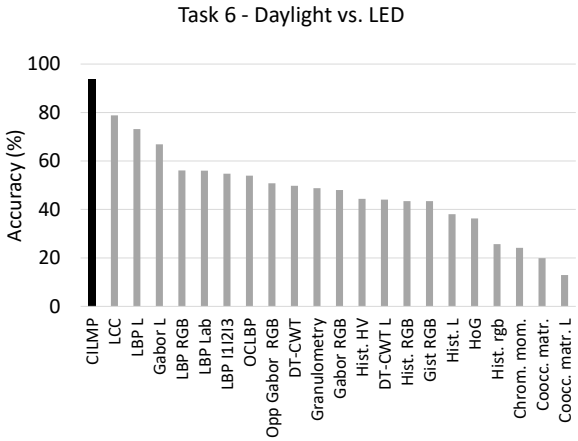

Figure 14: Average accuracy (%) obtained by CILMP and other texture descriptors for task 6.

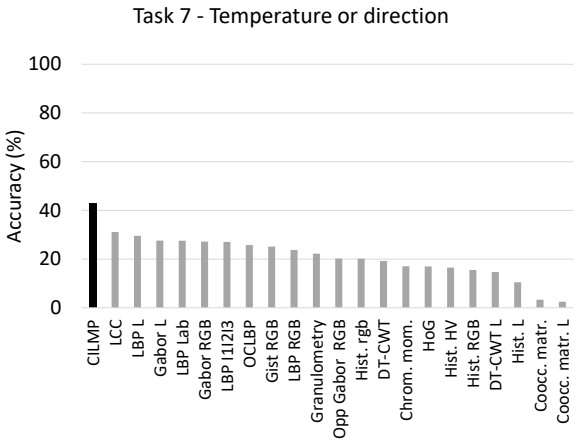

Figure 15: Average accuracy (%) obtained by CILMP and other texture descriptors for task 7.

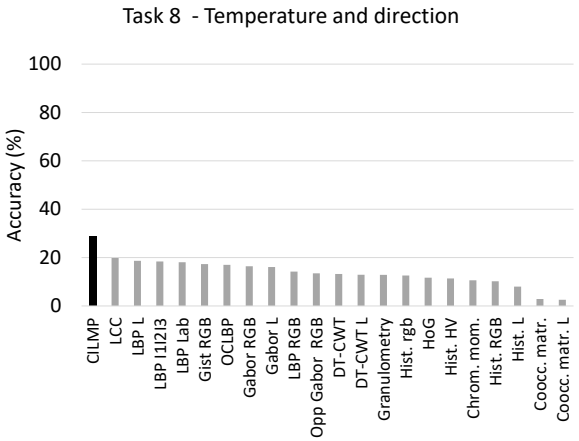

Figure 16: Average accuracy (%) obtained by CILMP and other texture descriptors for task 8.

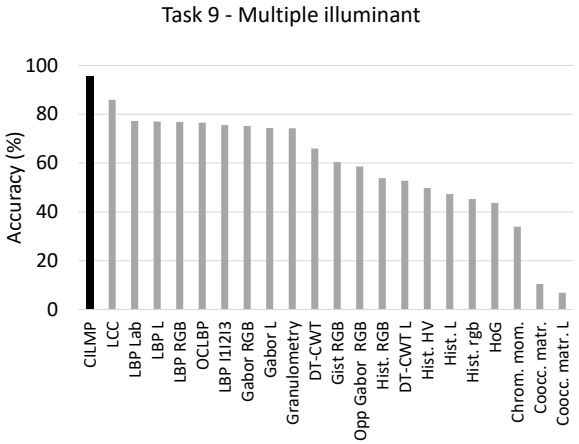

Figure 17: Average accuracy (%) obtained by CILMP and other texture descriptors for task 9 .

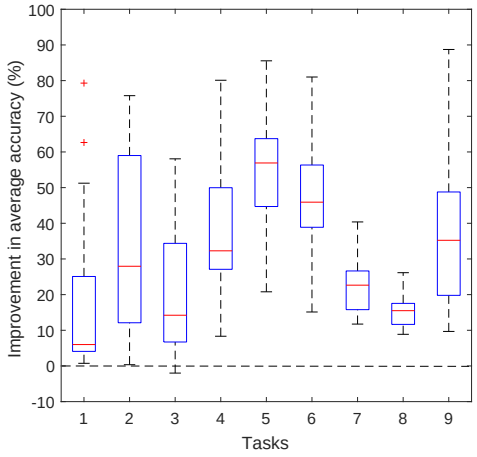

(a) Improvement obtained by CILMP in the average accuracy compared to the other descriptors.

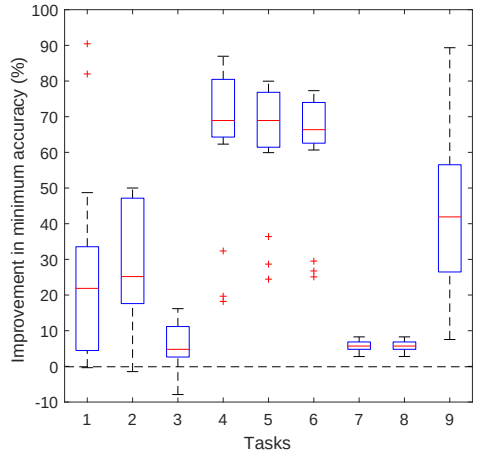

(b) Improvement obtained by CILMP in the minimum accuracy compared to the other descriptors.

Figure 18: Improvement achieved by CILMP for the nine tasks.

improvement in the average accuracy varies between 9.86% and 88.73%.

We notice from Fig. 18 that, in general, CILMP performs a large improvement over the other methods. The average improvement reached by CILMP is of 32.17% in the average accuracy and 34.49% in the minimum accuracy.

Finally, considering all the tasks, the rank reported in Table 3 shows that CILMP outperforms the existing descriptors. The complexity of CILMP, first in the rank, is similar to other methods, such as OCLBP and Opponent Gabor RGB, which have average rank of 5.89 and 10.89, respectively.

5 CONCLUSIONS

In this paper we have introduced a new color texture descriptor (CILMP) for texture classification under varying illumination. The proposed descriptor extends the local mapped pattern operator to color textures by combining color and texture information using multiresolution analysis. We applied a genetic algorithm to tune the descriptor parameters simultaneously.

We performed descriptor evaluation over nine tasks, which involve different cases of lighting changes. The results show that combining different resolutions of neighborhoods increases the classification accuracy. The complexity of CILMP is similar to others methods, and the proposed descriptor outperformed them for eight tasks and provided the 3*rd* best classification rate for the remaining task. CILMP reported an increase in average accuracy of up to 20.79% compared to the second-best method.

We also highlight that it is hard for all the methods to maintain high performance when the light source direction changes, and this is also a limitation of the proposed model. Thus, in future works, we plan to investigate how to make the descriptor invariant to changes in the light source direction, and we plan to evaluate other color spaces besides RGB to extract color information from texture.

ACKNOWLEDGEMENTS

The authors would like to thank the Sao Paulo Research Foundation (FAPESP), grant #2015/20812-5.

REFERENCES

Arvis, V., Debain, C., Berducat, M., and Benassi, A. (2004). Generalization of the cooccurrence matrix for colour images: application to colour texture classification. *Journal of Image Analysis and Stereology*, 23:63–72.

Bianconi, F., Harvey, R., Southam, P., and Fernández, A. (2011). Theoretical and experimental comparison of different approaches for color texture classification. *Journal of Electronic Imaging*, 20(4).

Campbell, N. W., Thomas, B. T., and Troscianko, T. (1996). Segmentation of natural images using self-organising feature maps. In *Proceedings of British Machine Vision Conference*, pages 223–232.

Chan, C. H., Kittler, J., and Messer, K. (2007). Multi-spectral local binary pattern histogram for component-based color face verification. In *First IEEE Int. Conf. Biometrics: Theory, Appl. and Systems*, pages 1–7.

Cusano, C., Napoletano, P., and Schettini, R. (2013). Illuminant invariant descriptors for color texture classification. In *Computational Color Imaging*, volume 7786 of *LNCS*, pages 239–249. Springer.

Cusano, C., Napoletano, P., and Schettini, R. (2014). Combining local binary patterns and local color contrast for texture classification under varying illumination. *J. Opt. Soc. Am. A*, 31(7):1453–1461.

Cusano, C., Napoletano, P., and Schettini, R. (2016). Evaluating color texture descriptors under large variations of controlled lighting conditions. *J. Opt. Soc. Am. A*, 33(1):17–30.

de Wouwer, G. V., Scheunders, P., Livens, S., and Dyck, D. V. (1999). Wavelet correlation signatures for color texture characterization. *Pattern Recognition*, 32(3):443 – 451.

Drimbarean, A. and Whelan, P. (2001). Experiments in colour texture analysis. *Pattern Recognition Letters*, 22(10):1161 – 1167.

Ferraz, C. T., Junior, O. P., and Gonzaga, A. (2014). Feature description based on center-symmetric local mapped patterns. In *Proceedings of the 29th Annual ACM Symposium on Applied Computing*, pages 39–44.

Gonzalez, R. C. and Woods, R. E. (2008). *Digital Image Processing (3rd Edition)*. Prentice-Hall, Upper Saddle River, NJ, USA.

Hanbury, A., Kandaswamy, U., and Adjeroh, D. A. (2005). Illumination-invariant morphological texture classification. In *Proceedings of the 7th Int. Symp. Mathematical Morphology*, pages 377–386.

Jain, A. and Healey, G. (1998). A multiscale representation including opponent color features for texture recognition. *IEEE Transactions on Image Processing*, 7(1):124–128.

Junior, O. L., Delgado, D., Goncalves, V., and Nunes, U. (2009). Trainable classifier-fusion schemes: An application to pedestrian detection. In *12th Int. IEEE Conf. Intell. Transp. Syst.*, pages 1–6.

Kandaswamy, U., Adjeroh, D. A., Schuckers, S., and Hanbury, A. (2012). Robust color texture features under varying illumination conditions. *IEEE Trans. Syst., Man, and Cybern., Part B: Cybernetics*, 42(1):58–68.

Maenpaa, T. and Pietikinen, M. (2004). Classification with color and texture: jointly or separately? *Pattern Recognition*, 37(8):1629 – 1640.

Ojala, T., Pietikainen, M., and Maenpaa, T. (2002). Multiresolution gray-scale and rotation invariant texture classification with local binary patterns. *IEEE Trans. Pattern Anal. Mach. Intell.*, 24(7):971–987.

Ojala, T., Pietikinen, M., and Harwood, D. (1996). A comparative study of texture measures with classification based on featured distributions. *Pattern Recognition*, 29(1):51 – 59.

Oliva, A. and Torralba, A. (2001). Modeling the shape of the scene: A holistic representation of the spatial envelope. *Int. J. Comput. Vision*, 42(3):145–175.

Palm, C. (2004). Color texture classification by integrative co-occurrence matrices. *Pattern Recognition*, 37(5):965 – 976.

Palm, C. and Lehmann, T. M. (2002). Classification of color textures by gabor filtering. *MG&V International Journal*, 11(2/3):195–219.

Paschos, G. (2000). Fast color texture recognition using chromaticity moments. *Pattern Recognition Letters*, 21(9):837 – 841.

Poirson, A. B. and Wandell, B. A. (1996). Pattern color separable pathways predict sensitivity to simple colored patterns. *Vision Research*, 36(4):515 – 526.

Sengur, A. (2008). Wavelet transform and adaptive neuro-fuzzy inference system for color texture classification. *Expert Systems with Applications*, 34(3):2120 – 2128.

Setchell, C. J. and Campbell, N. W. (1999). Using colour gabor texture features for scene understanding. In *7th International Conference on Image Processing and its Applications*, volume 1, pages 372–376.

Vadivel, A., Sural, S., and Majumdar, A. K. (2007). An integrated color and intensity co-occurrence matrix. *Pattern Recogn. Lett.*, 28(8):974–983.